JAERI-Tech
2000-023

STEERING OF HIGH ENERGY NEGATIVE ION BEAM AND DESIGN OF BEAM FOCUSING/DEFLECTION COMPENSATION FOR JT-60U LARGE NAGATIVE ION SOURCE

March 2000

Takashi INOUE, Kenji MIYAMOTO, Akihito NAGASE*,
Yoshikazu OKUMURA and Kazuhiro WATANABE

日本原子力研究所
Japan Atomic Energy Research Institute

本レポートは，日本原子力研究所が不定期に公刊している研究報告書です。
入手の問合わせは，日本原子力研究所研究情報部研究情報課（〒319－1195 茨城県那珂郡東海村）あて，お申し越しください。なお，このほかに財団法人原子力弘済会資料センター（〒319－1195 茨城県那珂郡東海村日本原子力研究所内）で複写による実費頒布をおこなっております。

This report is issued irregularly.
Inquiries about availability of the reports should be addressed to Research Information Division, Department of Intellectual Resources, Japan Atomic Energy Research Institute, Tokai-mura, Naka-gun, Ibaraki-ken 〒319－1195, Japan.

編集兼発行　日本原子力研究所

Steering of High Energy Negative Ion Beam and Design of Beam Focusing/Deflection Compensation for JT-60U Large Negative Ion Source

Takashi INOUE, Kenji MIYAMOTO[+], Akihito NAGASE[*],
Yoshikazu OKUMURA[+] and Kazuhiro WATANABE[+]

Department of ITER Project
Naka Fusion Research Establishment
Japan Atomic Energy Research Institute
Naka-machi, Naka-gun, Ibaraki-ken

(Received February 3, 2000)

A large negative ion source for JT-60U produces high current ion beam from a wide extraction area of 45 cm x 110 cm. On the other hand, a cross-sectional area of the negative ion based neutral beam (NNB) injection port on JT-60U is narrow, about 50 cm x 60 cm. In order to inject the neutral beam at a high geometric efficiency, i.e. to suppress beam loss in the beamline, it is necessary to steer the beam for both compensation of undesirable beam deflection in extractor and focusing of the beam. For the JT-60U, two methods are provided for the required beam steering. Among them the results of beam steering experiment by aperture displacement and the design study are summarized in the present report. The experiment was carried out with 400 keV negative ion source, which has the three stage accelerator of similar structure as the JT-60U ion source, at Negative Ion Acceleration Test Stand (NIAS). High energy negative ion beams of the same perveance as that of 500 keV full power operation of the JT-60U ion source were steered with displacement of electron suppression grid and grounded grid for the beam deflection compensation and the focusing. The experimental results of the high energy beam steering are discussed based on the thin lens theory. Then the aperture arrangement of electron suppression grid and grounded grid are designed for the large negative ion source of JT-60U NNB injector.

Keywords : Nuclear Fusion, JT-60, Neutral Beam, NBI, H^-Ion, Accelerator, Ion Beam, Beam Optics, Thin Lens Theory, Beam Focussing

---

[+] Department of Nuclear Fusion Engineering

[*] Hitachi Co. Ltd.

高エネルギー負イオンビームの偏向実験と JT-60U 負イオン源のビーム集束・磁場偏向補正の設計

日本原子力研究所那珂研究所 ITER 開発室
井上多加志・宮本 賢治+・永瀬 昭仁*・奥村 義和+・渡辺 和弘+

（2000 年 2 月 3 日受理）

JT-60U 大型負イオン源は 45 cm x 110 cm という大面積引き出し面から大電流負イオンビームを生成する。一方、JT-60U の N-NBI 入射ポートのビーム通過部最小断面は約 60 cm x 50 cm と狭小であり、ビームラインでのビーム損失を抑え高い幾何学的効率で中性粒子ビームを入射するためには、加速管内での不整なビーム偏向を補正しかつビームを集束する必要がある。JT-60U 大型負イオン源ではこのビーム集束の要件を満たすため、２つのビーム集束法を用いる。本報告は、このうち電極孔変位（孔ズレ）によるビーム偏向について行った実験と設計検討の結果をまとめたものである。実験は JT-60U 大型負イオン源と同等の３段加速構造をもつ負イオン加速試験装置 NIAS の 400 keV 負イオン源を用いて行った。電子抑制用磁場によるビーム偏向の補正のために電子抑制電極を、またビーム集束のために接地電極を変位させ、JT-60U 大型負イオン源の 500 keV 22 A のフルパワー運転と同じパービアンスを保ってビーム偏向を行った。この結果を検討し、JT-60U 大型負イオン源の電子抑制電極・接地電極の電極孔パターン設計を確定したものである。

那珂研究所：〒311-0193 茨城県那珂郡那珂町向山 801-1
+ 核融合工学部
*（株）日立製作所

Contents

1. Introduction..... 1

2. Experimental Setup..... 2

3. Result and Discussion..... 3
3.1 Beamlet Profile Measurement..... 3
3.2 Beamlet Steering by Aperture Displacement in GRG 4
3.3 Beamlet Deflection by Magnetic Field in EXG 6
3.4 Beamlet Steering by Aperture Displacement in ESG 7

4. Design of Aperture Displacement for JT-60U Source..... 8
4.1 Design Concept..... 8
4.2 Displacement in GRG for Beam Focusing..... 9
4.3 Displacement in ESG for Compensation of Deflection..... 10

5. Summary 10

Acknowledgment 11

References 12

目次

1. はじめに 1

2. 実験装置 2

3. 実験結果 3
3.1 ビーム分布測定 3
3.2 接地電極変位によるビーム偏向 4
3.3 引出し電極内磁場によるビーム偏向 6
3.4 電子抑制電極変位によるビーム偏向 7

4. N-NBI 負イオン源接地電極の設計 8
4.1 設計の方針 8
4.2 ビーム集束のための接地電極変位 9
4.3 磁場によるビーム偏向補正のための電子抑制電極変位 10

5. まとめ 10

謝辞 11

参考文献 12

1. INTRODUCTION

The large negative ion source for JT-60U produces high current ion beam from a wide extraction area of 45 cm x 110 cm. On the other hand, a cross-sectional area of negative ion based neutral beam (N-NB) injection port on JT-60U is narrow, about 50 cm x 60 cm in the area. There are two issues to inject the neutral beam at a high geometric efficiency. One is to focus the beam produced from the wide grid area into the narrow port. The other is to compensate an undesirable beam deflection due to magnetic field in the extractor. In order to suppress beam loss in the beamline, beam steering is necessary for both focussing and the compensation of the deflection. In JT-60U ion source two methods are provided for the required beam steering.

The large extraction/acceleration grids of the JT-60U ion source are divided into five segments. Each segment of which dimension is 45 cm wide and 18 cm long is lined up vertically to compose the wide extraction/acceleration area. The center segment is adjusted to emit the beam in parallel to the beamline axis. The two neighbor segments are 0.5° inclined with respect to the center segment. Next two outer segments are 0.5° inclined further. Then the beam is fired straightforward so as to be focused at 28 m downstream from the source. This is the primary method of the beam focusing, what is called as 'geometric focus', adopted in the JT-60U ion source. The geometric focal point of the real JT-60U ion source was already verified using a laser assisted aperture alignment device.

Another method is the steering of beamlet by aperture displacement, which have been widely used in the existing positive ion based NB systems [1, 2, 3, 4]. The steering of negative ion beam [5, 6] was examined and characterized with the source composed of an extractor and a single stage accelerator at high current negative ion source test stand (ITS-2M). Based on the results obtained in the single stage accelerator, design of the beam focusing was studied as described in the design report of JT-60U N-NBI[7].

In the earlier experiment at ITS-2M, fine beamlets of which divergence was nearly 5 mrad were obtained by optimizing the beam optics. Consequently negative ion deflection due to magnetic field in the extractor was found by measuring precise position of each beamlet downstream. In JAERI electrostatic extractor small permanent magnets are embedded between apertures to form a dipole magnetic field in the extraction gap. This magnetic field is utilized for electron suppression accompanying the ions. Since the magnets are arranged in alternative polarity in each aperture row, negative ions are deflected in the alternative direction line by line. The beam deflection

angle ranging from 5 to 10 mrad was observed. In this series of experiment, it was demonstrated that the beamlet deflection due to the magnetic field could be compensated with beamlet steering by aperture displacement in the electron suppression grid.

Objectives of the present experiment were:

1) to demonstrate the high energy negative ion beam steering with the three stage accelerator of similar structure as the JT-60U ion source.
2) to characterize the beamlet steering by aperture displacement in the accelerator of this structure.
3) to determine reasonable displacement for the JT-60U ion source for both beam focusing and the deflection compensation.

The present report describes the steering of the high energy beam by aperture displacement and its application for the JT-60U ion source. The experiment was carried out with 400 keV negative ion source, at Negative Ion Acceleration Test Stand (NIAS). High energy negative ion beams of the same perveance as that of the JT-60U source at the full power operation (500 keV 22 A) were steered with displacement of electron suppression grid and grounded grid for the beam deflection compensation and the focusing. The experimental results of the high energy beam steering were discussed based on the thin lens theory. Then the aperture arrangement of electron suppression grid and grounded grid are determined for JT-60U ion source.

2. EXPERIMENTAL SETUP

A cross sectional view of "400keV negative ion source" used in the present experiment is show in Fig. 1. The extractor/accelerator has the similar structure [8] as the JT-60U source to simulate high energy acceleration of JT-60U NNBI. The schematic of the extractor/accelerator grids is also illustrated in Fig. 2 with the electric wiring. Three grids in the extractor are called as plasma grid (PLG), extraction grid (EXG), and electron suppression grid (ESG), as shown in the figure. The negative ions produced in KAMABOKO plasma generator [9] are extracted from the extractor apertures of which diameter are 14 mm. The accelerator is a three stage electrostatic accelerator consists of three grids, named A1G, A2G and GRG, to downstream respectively. The extractor and each grid in the accelerator are placed so that the acceleration gap is to be 75 mm, 65 mm and 55 mm in between. The aperture diameter

in the accelerator grids is 16 mmϕ. These parameters concerning beam optics were taken to be equivalent as those of JT-60U source [10]. The 400 kV DC high voltage applied for the acceleration is sustained with three insulator columns made of filament winding type fiber reinforced plastic.

The grid aperture arrangements in ESG and GRG with displacement are illustrated in Fig.3 and 4, respectively. Out of 49 apertures arranged in 7 x 7 array, "E" shaped pattern of apertures in the top, center, bottom lines and the left column were kept aligned so as to produce unsteered beamlets. The rest of apertures, i.e. in second, third, fifth and sixth lines from the top of the illustration, were displaced with respect to apertures in the other grids. The polarity of the magnets embedded in EXG is superimposed in left hand side of the Fig.3. As shown in the figure, the polarity changes alternatively line by line. Hence the beamlets extracted from apertures in second and third lines are deflected in opposite direction each other due to the alternative polarity. The beamlets from apertures in fifth and sixth lines are also deflected as the same manner. The beamlet steering was observed with displacing the apertures every 0.2mm up to 1.0 mm in ESG, and every 1.0 mm up to 6.0 mm in GRG in the present experiment. (Accuracy of the aperture machining and assembly is less than 0.05 mm.)

The intermediate voltages for the three stage acceleration were supplied from voltage divider consisted of a series resistor at NIAS. Hence the voltage is perturbated if much beam current (~ 0.1 A) is flowed in the grids with respect to the breeder resister current (0.5 A). To avoid this voltage perturbation, the beam was extracted only from fourteen apertures in two lines, an aligned and a displaced aperture lines, out of 49 aperture array. Then the other apertures were masked during the series of experiment. This enabled us to operate the source at the same perveance as that of 500 keV, 22 A operation of JT-60U source.

The beamlet profile and the precise position were measured by observing the light emitted from interaction of beam and residual gas in the beamline with a video monitor located 1581 mm downstream from GRG of the source.

3. RESULT AND DISCUSSION

3.1 Beamlet profile measurement

An example of the measurement with the video monitor is shown in Fig. 5. The figure shows the beamlet profiles produced from two apertures in an aligned line. Since reflected light from background and the beam plasma is also measured in the video, the

beamlet profile becomes a relatively broad one than the real beamlet. The beamlet divergence was in a range of 8 ~ 9 mrad through the present experiment.

A profile of the beamlets produced from a line of aligned apertures is shown in Fig. 6. The aperture pitch between the aligned apertures is 19 mm as shown in Fig. 3 and 4. However, the measured beamlet pitch was wider than the apertures pitch in particular in the peripheral beamlets. This indicates that beamlets produced from aligned apertures are already deflected. Due to extruded grid support structure from the grounded flange into the 400 keV accelerator, the electric field around the grounded grid is distorted so much. The electrostatic field between the grids is spherically curved so as to smoothly trace the grid and the support shape. Although a metal ring (See Fig. 1) was installed around the grid to form a parallel field between the grids, it resulted in a slight over-compensation to form a concave field. This is the reason why the aligned beamlets are measured with the wider pitch.

The measured profiles obtained with the video monitor contained many noise spikes as shown in Fig. 6. The more spikes were observed in the production of higher power beam. The origin of the noise is supposed as the bremsstrahlung caused by acceleration of electrons [11]. The beam profile was obtained several times at a series of beam operation. Then an average of the beamlet pitches was examined in the present experiment so that the error due to the noise did not affect to the measurements.

3.2 Beamlet steering by aperture displacement in GRG

Among aperture arrangement shown in Fig. 4, center aperture line (4th line; aligned) and its upper and lower lines (3rd and 5th lines; displaced) were measured in the present experiment. A result of the beamlet measurement produced from the GRG displaced apertures are shown in Fig. 7. As in the figure, the distances between each beamlet are expanded than those of aligned beamlets in Fig. 6. This is due to the beamlet steering by aperture displacement. The steering angle was obtained by comparing the beamlet pitches produced from aligned and displaced apertures.

The steering angle observed at beam energy of 310 keV is shown in Fig. 8 as a function of the aperture displacement. The sign of the abscissa (direction of displacement) was taken to be plus if an aperture is displaced in the same direction as the magnetic deflection. (Note that a beam produced from the aperture displaced in plus direction is steered in minus direction in ESG. That is, both steering and deflection take place in the same direction if displaced in minus direction.) An analytical result obtained with the thin lens theory ($\theta = 0.00164\ \delta$, θ: steering angle, δ: displacement) is

also drawn in the figure. Findings here can be summarized as follows:

1) Deviations of the experimental results obtained with displacement of ±1 mm and ±4 mm are due to the distorted electric field near the compensation ring.
2) The experimental data show slightly larger steering angle than the analysis. This is due to an effect of finite thickness of the actual grid, where electric field penetrates deeply into the thick aperture. The electric field in the aperture is deformed with an unpredicted small curvature. Then the beamlet are steered with a large angle by the electric field of small curvature.
3) The steering angle is lager in steering of minus direction than plus direction. This is supposed that the uncompensated magnetic deflection slightly affected in the steering in the GRG.
4) Considering above discussions, it is concluded that the experimental data show almost good agreement with the analytical result.

The above results are obtained with beam optics keeping the same as that of the JT-60U ion source. Also one thing it should be noted is that the beam steering by the GRG displacement is not affected so much to the beam energy. From these it is expected that the steering by the aperture displacement is effective for focusing of the JT-60U N-NBI negative ion beam.

As described in the design report [7], it is necessary to displace aperture so much to focus the whole beam produced from the wide grid of JT-60U source to a focal point in the narrow port. However it was anticipated that the high energy beam was intercepted by the grid due to so much aperture displacement. Even if the beam does not intercepted it might suffer deterioration of the beam quality due to the irregular electric field curvature in the aperture peripherals.

In the beam profile shown in Fig. 7, the left side peak indicates a beamlet produced from aligned aperture, then the others are the steered beamlets. The right hand side beamlet, which suffered the displacement of 6 mm, looks like having a broadened profile. It was found that the beamlet divergence produced from aperture displacement more than 4 mm was larger than those obtained with smaller displacement.

The beamlet divergence obtained from aligned and displaced (δ = 4 mm) apertures in GRG are shown in Fig. 9 as functions of negative ion current density. At the perveance equivalent to the full power operation of JT-60U source (310 keV、JH^- = 9 mA/cm^2), the divergence of beamlets produced from displaced apertures of up to 4 mm is the same as that obtained from the aligned aperture. Since the perveance curve is

almost the same with and without displacement up to 4 mm, it is also considered that the steered beamlets did not hit the grid. (The steered beamlets showed a smaller divergence at the current lower than that giving the minimum divergence in aligned beamlets. This is because that those peripherals of steered beamlet are cut due to interception at the mismatched perveance.) It is concluded that the aperture displacement should be limited by 4 mm in GRG for the application to the JT-60U ion source.

3.3 Beamlet deflection by magnetic field in EXG

The center and bottom aperture lines, where the apertures were aligned as shown in Fig. 3, have an opposite polarity of magnetic field. Then the beamlets produced from these apertures are deflected in the opposite direction each other. Fig. 10 shows a result of the deflection angle measured at various beam energies. The deflection angles produced from each column of the aligned aperture lines are shown in the figure. The data points are scattered so much. This is due to beam deflection by curved electric field in the extruded grid support structure as mentioned in section 3.1. Both deflections due to the magnetic field and the curved electric field are appeared in the figure. In order to look only at the magnetic deflection, the unfavorable effect of electric field must be eliminated. The column E (See right hand side of Fig. 10) is located in the center column of the aperture arrangement, where the electric field is expected to be parallel to the grids. Hence the data of column E is considered to be most reliable. Hereafter the data on column E are referred to the following discussion.

Fig. 11 presents a log plot of the result of Fig. 10. The data points obtained in column E is shown in open circle. The data obtained in earlier experiment [5, 6] with 10 A (ten ampere) source is also shown in open triangle in the figure. The magnet for electron suppression used in 10 A source was 2.7 mm x 4.7 mm in the cross-sectional area. Whilst the magnets size in both 400 keV source and JT-60U source are twice larger, 5.4 mm x 4.7 mm in the cross-section.

From Larmor gyro radius of ions in a magnetic field, the beamlet deflection angle φ is proportional to:

$$\varphi \sim Bl/\sqrt{E} \qquad (1)$$

Here,

Magnetic flux: B

Distance of effective magnetic field: l
Beam energy in the magnetic field: E

The magnets of 400 keV source and JT-60U source form the magnetic field of twice lager "Bl" than that of 10 A source. For a direct comparison the result obtained from 10 A source is multiplied by two and shown in closed triangle.

As in the formula (1) the deflection angle is proportional to -1/2th power of the beam energy. The data indicated with triangle reaches to the line proportional to $E^{-1/2}$ asymptotically in low energy range. Whilst the deflection angle decreased further than the $E^{-1/2}$ dependency. This is an effect of axial acceleration and beam steering at GRG in the single stage accelerator.

The result obtained in the present experiment show the $E^{-1/2}$ dependency except for the data obtained at 160 keV. If we extrapolate the present result to 500 keV full acceleration of JT-60U source, the deflection angle is predicted to be 5 mrad.

3.4 Beamlet steering by aperture displacement in ESG

Steering angle with ESG displacement was measured in the energy range of 160 ~ 300 keV. The steering angle is shown in Fig. 12 as a function of the displacement for various beam energies. The data points are scattered as well as those of deflection. This is again due to the curved electric field. Hence the results with displacement of 0.2 mm and 1.2 mm, which were arranged in peripherals of the grid aperture arrangement, are not reliable. The fitting line in the figure, which was drawn considering these discussions, shows that the steering angle is almost proportional to the displacement.

The steering angle for unit displacement is obtained as presented in Fig. 13 from slopes of the fitting line in Fig. 12. The steering angle per unit displacement increases with the energy and shows saturation at the high energy regime. The steering angle at 300 keV is about 8 mrad/displacement in mm. (The energy dependence of the steering angle is also plotted in Fig. 11 in closed circle with the results of deflection.)

In the thin lens theory adopted in the extractor/single stage accelerator, the steering angle by ESG displacement is derived as follows;

$$\theta_{ESG} = \left(\frac{Vext}{Vext + Vacc1}\right)^{1/2} \frac{\delta_{ESG}}{F_{acc1}} \qquad (2)$$

Where,

Vext: Extraction voltage
Vacc1: Acceleration voltage applied between ESG and A1G
θ_{ESG}: Displacement in ESG
Facc1: Focal length of electrostatic lens in ESG, given as

$$Facc1 = 4Vext / (Eacc1 - Eext) \quad (3)$$

Eacc1 and Eext are electric field in first acceleration gap (gap length: dacc1) and extraction gap (gap length: dext), respectively. Now it is obvious that it is not appropriate to adopt the thin lens approximation for the ESG lens, since EXG seems thick enough to isolate the ESG lens from electric field in the extraction gap, Eext. Then neglecting Eext as a first order approximation, the focal length, Facc1, is simply given as;

$$F_{acc1} \sim \frac{4\,V_{ext}}{E_{acc1}} = \frac{4\,V_{ext}}{V_{acc1}}\, d_{acc1} \quad (4)$$

Then substituting the formula (4) into the formula (2), we obtain proportional relation between θ_{ESG} and δ_{ESG}:

$$\frac{\theta_{ESG}}{\delta_{ESG}} \approx \left(\frac{1}{1 + \frac{V_{acc1}}{V_{ext}}} \right)^{\frac{1}{2}} \frac{1}{4} \frac{V_{acc1}}{V_{ext}}\, d_{acc1} \quad (5)$$

In the present experiment the ratio Vext/Vacc1 was kept constant to produce the beam at the same perveance as the JT-60U ion source. Thus the steering angle at ESG is predicted to be independent of the beam energy from the thin lens theory. This suggests a good agreement of the analysis with the saturation tendency of the steering angle observed at higher energy range. Here it is concluded that the steering angle of about 8 mrad/mm is expected by ESG displacement in the energy range above 300 keV to 500 keV.

4. DESIGN OF APERTURE DISPLACEMENT FOR JT-60U SOURCE

4.1 Design concept

Almost ten years ago, it took several years to achieve high reliability in positive-ion-based NB system. At JET NBI [2] one of the initial troubles was in the beam steering by the aperture displacement. They adopted the linear optics theory directory into deceleration grid of PINI source. The deceleration grid was thick enough to immerse the deceleration electric field in the aperture to suppress the backstream electron. As the result, the analysis based on the thin lens assumption gave an underestimation in the steering angle; i.e. the beams were over focused. Then the beam caused a high heat flux in the beamline. Generally the over focused beam causes a higher heat flux in the beamline than in a case of under focus. For JT-60U source this experience was also utilized in the present design.

1) The steering angle to be obtained in the JT-60U source is assumed as 1.5 times larger than the analysis.

In the GRG displacement, the present experiment showed 20 % larger steering angle than the analysis. One of the reasons to this is considered due to the finite thickness of the real grids. Further, the GRG thickness of JT-60U source (20 mm) is thicker than the grid used in the present experiment (10 mm). Another point that should be mentioned is that the grid in the JT-60U source has a 45° cut around the aperture. This cut allows the electric field immerse deeply into the aperture, consequently the beam is steered more than that without the cut by the deeply penetrated curved field in the aperture.

2) As for GRG design, the beams are steered so as to be focused on a segment axis at 28 m downstream. Whilst the maximum displacement should be limited by 4mm.

In the shorter direction of the GRG segment, the apertures are displaced so that the beams are steered and focused on the segment axis at 28 m downstream. Then the apertures are displaced as large as possible in the longer direction of the segment within the limit of total displacement of 4 mm.

4.2 Displacement in GRG for beam focusing

Based on the experimental result and discussion above, the aperture arrangement of GRG in the JT-60U source was designed as shown in Fig. 14. The

figure indicates how the apertures are displaced as the position in a segment. The pitches of the apertures in aligned grids are 21 mm in shorter direction of the segment, and 19 mm in the longer direction. Then the apertures in GRG are displaced so that the pitches are 21.3 mm (shorter direction) and 19.3 mm (longer direction).

Outside of the aperture area for the beam production, four supplemental apertures are drilled on the corner for the alignment of the segment. The apertures for beam and alignment would be overlapped each other on the corner of the peripheral arrangement, if the wider pitch was adapted to all apertures in longer direction. Displacement of each two apertures next to the alignment apertures is reduced properly.

The originally designed focal point was 23660 mm from the source. According to the present design, the new focal point is estimated to be 28 m downstream from the source, inside of JT-60U vacuum vessel. With this focal length the heat load in the beamline was already evaluated to be blow a permissible level [12].

4.3 Displacement in ESG for compensation of deflection

From the result and discussion in section 3.3, required ESG displacement to compensate the magnetic deflection is given as follows,

$$\frac{(\text{Deflection angle by magnetic field (rad)})}{(\text{Steering angle by unit displacement (rad/mm)})} = 0.6 \text{ mm} \quad (6)$$

Here, considering the concept 1) in the section 4.1, the displacement of ESG was decided to be 0.5 mm. The aperture arrangement of ESG in a segment is designed as shown in Fig. 15 for the JT-60U source.

5. Summary

Steering of high energy beam by aperture displacement was studied using 400 keV negative ion source at NIAS, which has a similar three stage accelerator as the JT-60U large negative ion source. Based on the experimental result, aperture arrangement of electron suppression grid (ESG) and grounded grid (GRG) were designed for JT-60U ion source.

(1) The steering angle obtained with grounded grid displacement showed almost good agreement with the analytical result based on the thin lens theory. At the perveance equivalent to the full power operation of the JT-60U source (310 keV、JH^- = 9 mA/cm^2), the divergence of beamlets produced from displaced apertures of up to 4 mm is the same as that of the aligned aperture. It was confirmed that the steered beamlets did not hit the grid if the aperture displacement is limited by 4 mm in GRG.

(2) Both the steering and deflection angles showed a -1/2th power dependency on the beam energy. If we extrapolate the present result to 500 keV full acceleration of the JT-60U source, the deflection angle is predicted to be 5 mrad. The steering angle at 500 keV is expected to be about 8.25 mrad/unit displacement in milli-meter.

(3) Considering the finite thickness of the real grid, the steering angle by GRG displacement to be obtained in the JT-60U source was assumed as 1.5 times larger than the analysis. Then the apertures in GRG were displaced so that the aperture pitches are 21.3 mm (aligned: 21 mm) in shorter direction and 19.3 mm (aligned: 19 mm) in longer direction.

(4) The displacement of ESG in JT-60U source was decided to be 0.5 mm for compensation of the magnetic deflection.

Acknowledgment

The negative ion acceleration test stand (NIAS) was assigned for the present experiment for a month, in midsummer 1994. In order to terminate the experiment within the period, and also to catch up with manufacturing of the JT-60U ion source accelerator section, the experiment had been carried out vigorously.

In such a rushing schedule, the present displacement would not be designed with a high reliability if the experience of positive-ion-based NBI had not been sufficiently available. The authors would like to thank Dr. Ohara, who gave us fruitful comments and discussions based on the positive ion beam experience. Also the present experiment and design were completed through supports from staffs in the NBI Heating Laboratory and the NBI Facility Division. They are grateful to Dr. Y. Seki, Dr. T. Tsunematsu, Dr. A. Kitsunezaki, and Dr. S. Matsuda for continuous encouragement s and supports.

References

[1] M. Kuriyama et al., "The design, Research and Development of JT-60 Neutral Beam Injector" (in Japanese), JAERI-M 87-169, Oct. (1987).

[2] G. Duesing, Fusion Technology 1984 (Proc. of 13th SOFE), CEC/Pergamon press, Volume 1 p. 59, Varese, Sept. 24-28 (1984).

[3]Y. Okumura et al., Rev. Sci. Instrum. 51/4, 471 (1980)

[4]Y. Ohara, Japanese J. Appl. Phys., 18/2, 351 (1979)

[5] T. Inoue, "Steering of H^- Beamlet by Aperture Displacement", Proc. IAEA Technical Committee Meeting on Negative Ion Based Neutral Beam Injectors p.189, JAERI Naka, Nov. 11-13 (1991).

[6] T. Inoue et.al., "Steering of H- Beamlet by Aperture Displacement", to be appeared in Japan Atomic Energy Research Institute report, JAERI-Tech (1999).

[7] NBI Facility Division, NBI Heating Laboratory, "Design study of a negative-ion based NBI system for JT-60U" (in Japanese), JAERI-M 94-072, March, 1994.

[8] K. Miyamoto et.al., "Development of a 400 keV multistage electrostatic accelerator for neutral beam injectors", Proc. 16th SOFT, Karlsluhe, Aug. 22-26 (1994).

[9] T. Inoue et.al., "Merging pre-accelerator for high current H^- ion beams", to be appeared in Rev. Sci. Instrum. July (1995).

[10] Y. Okumura et.al., Proc. 6th Int. Symp. on Production and Neutralization of Negative Ions and beams, AIP Conf. Proc. No. 287, 839, Upton NY, Nov. (1992).

[11] M. Mizuno et.al., Proc. 6th Int. Symp. on Production and Neutralization of Negative Ions and beams, AIP Conf. Proc. No. 287, 710, Upton NY, Nov. (1992).

[12] M. Kazawa, "Heat load on the N-NBI beam limiter" (in Japanese), Internal memo of NBI Facility Division, 21 September, 1994.

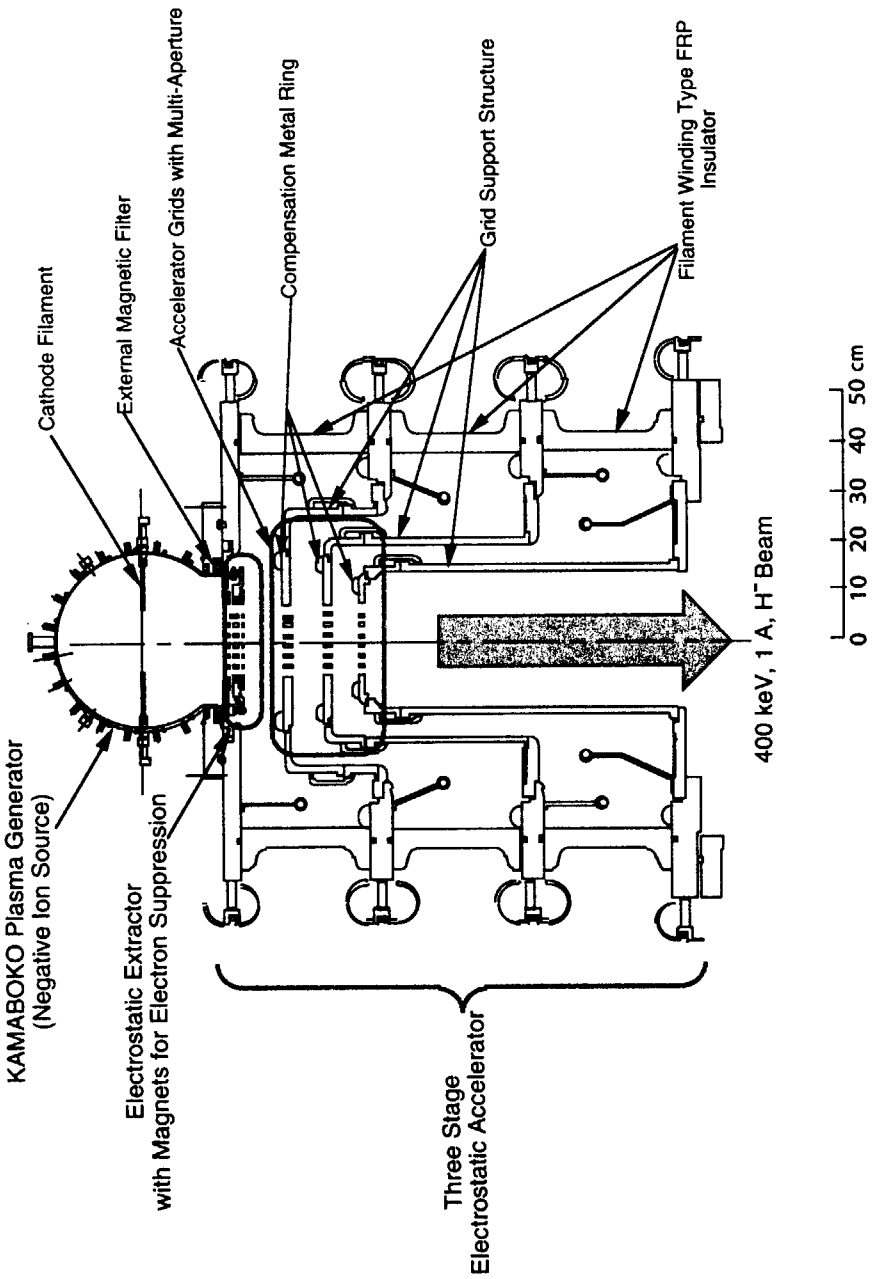

Fig. 1. A cross-sectional view of "400 keV negative ion source" at NIAS.

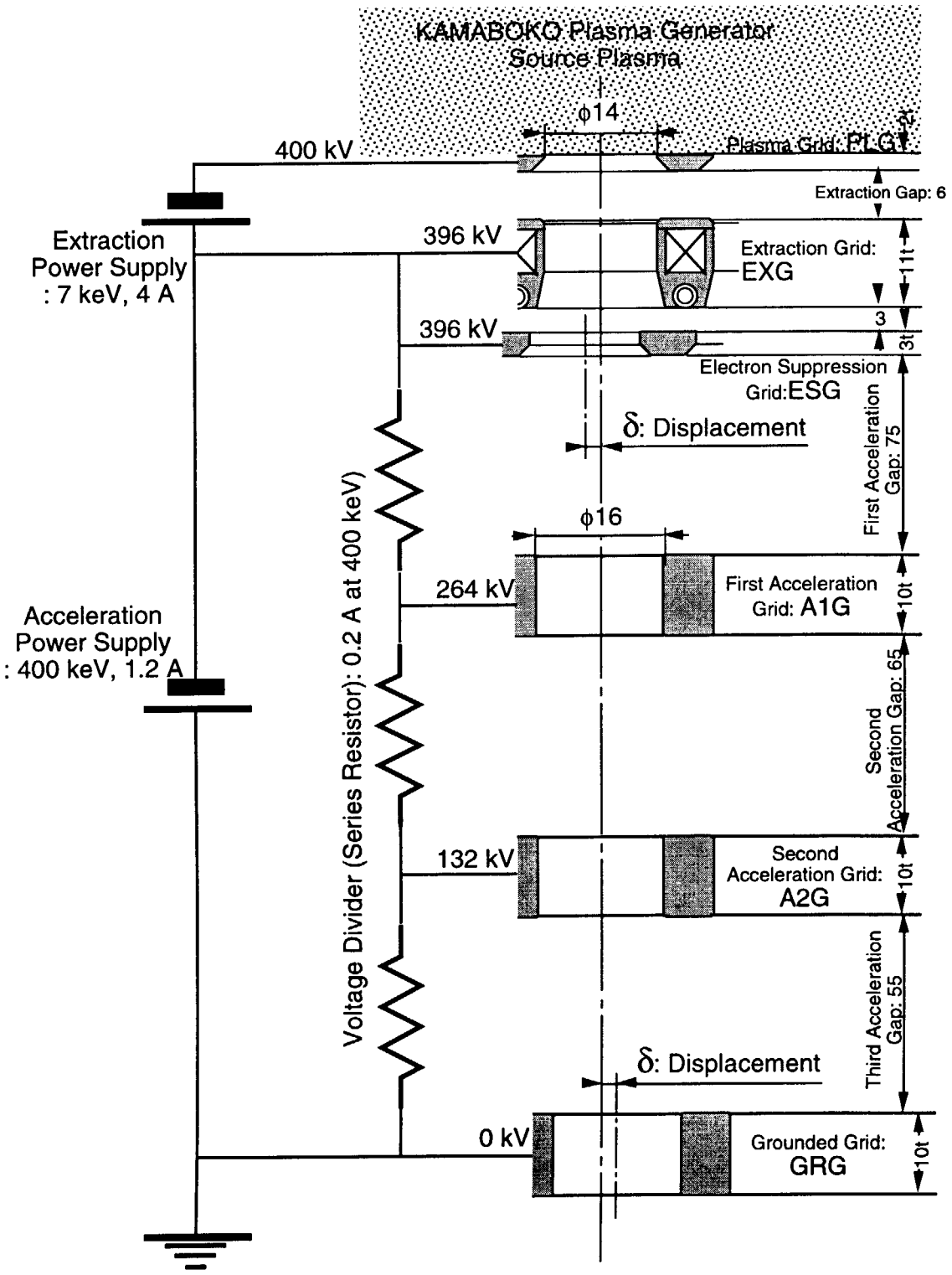

Fig. 2. A schematic of the extractor/accelerator grids in 400 keV negative ion source with the elecric wiring.

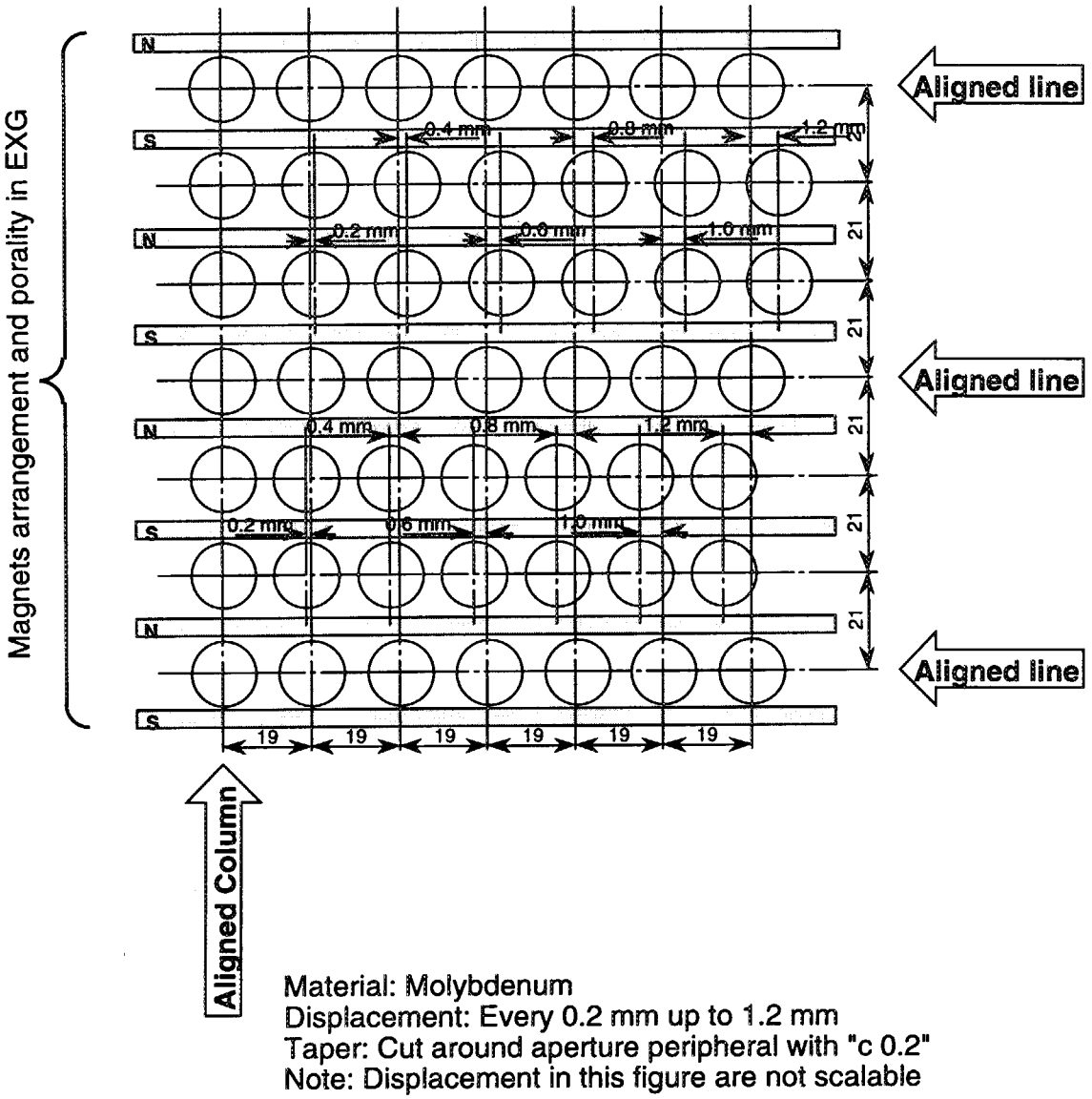

Fig. 3. An illustration of grid aperture arrangement in ESG.

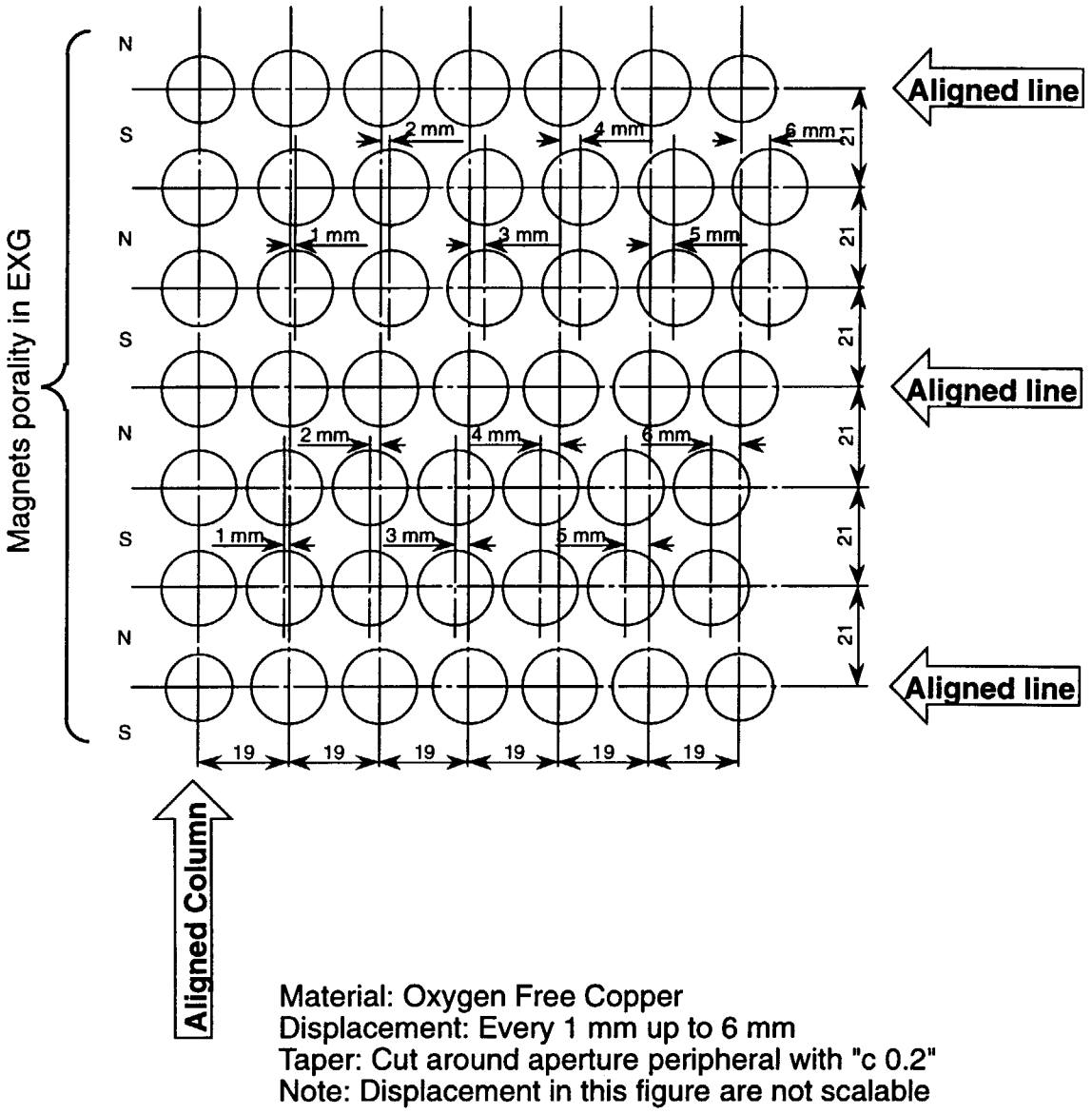

Fig. 4. An illustration of grid aperture arrangement in GRG.

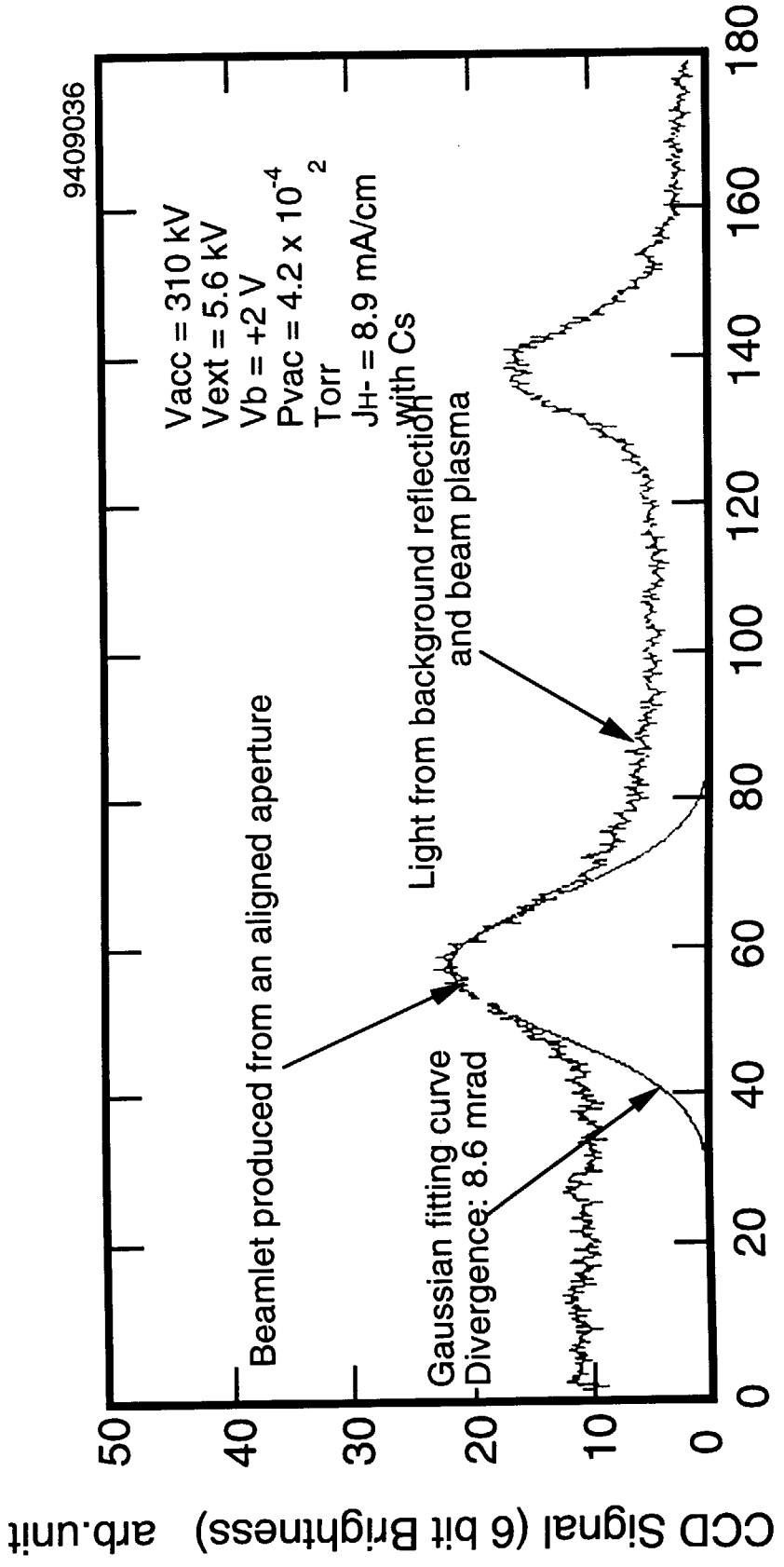

Fig. 5. An example of beamlet profile produced from an aligned single aperture.

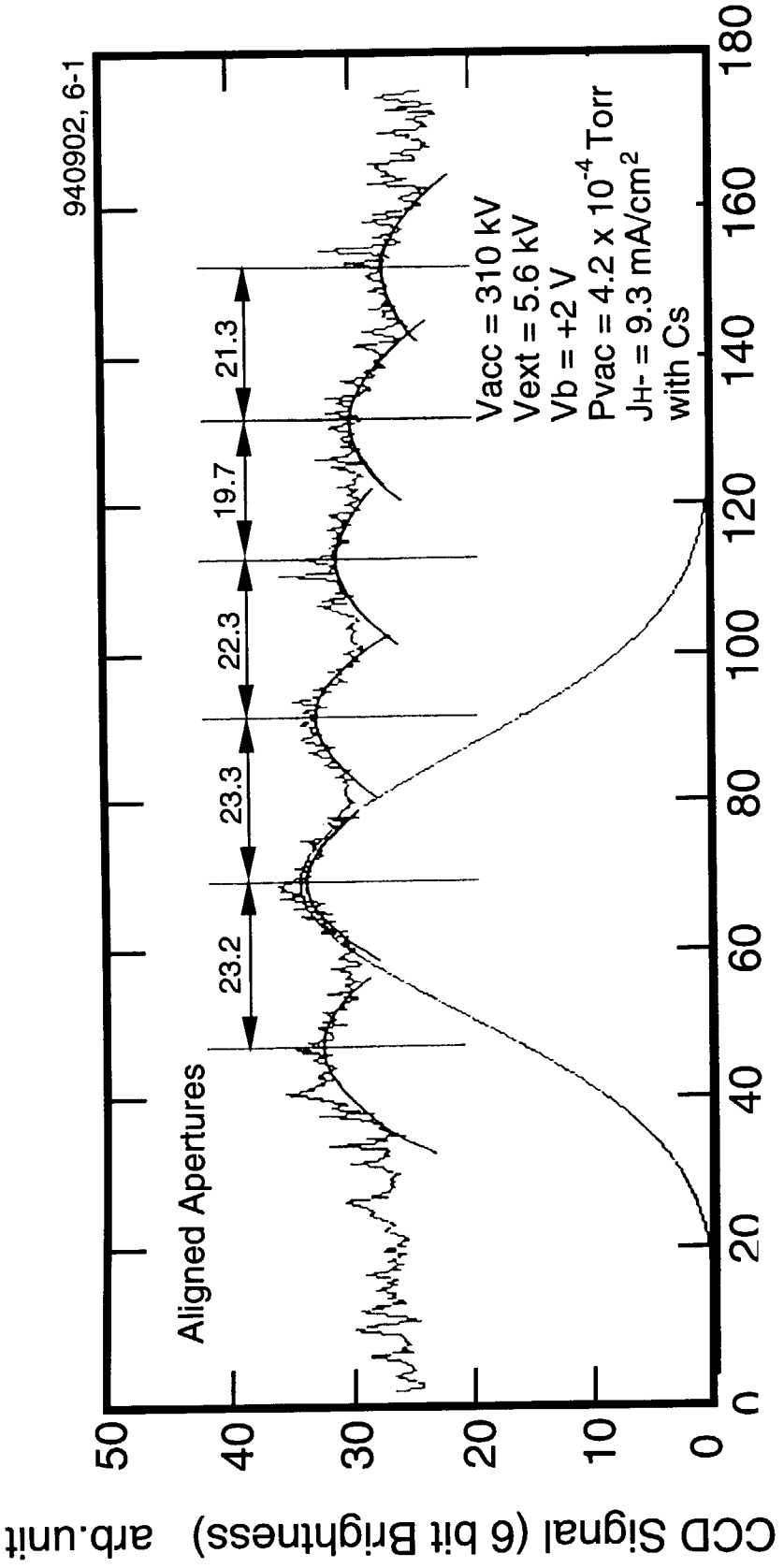

Fig. 6. A profile of the beamlets produced from a line of aligned apertures.

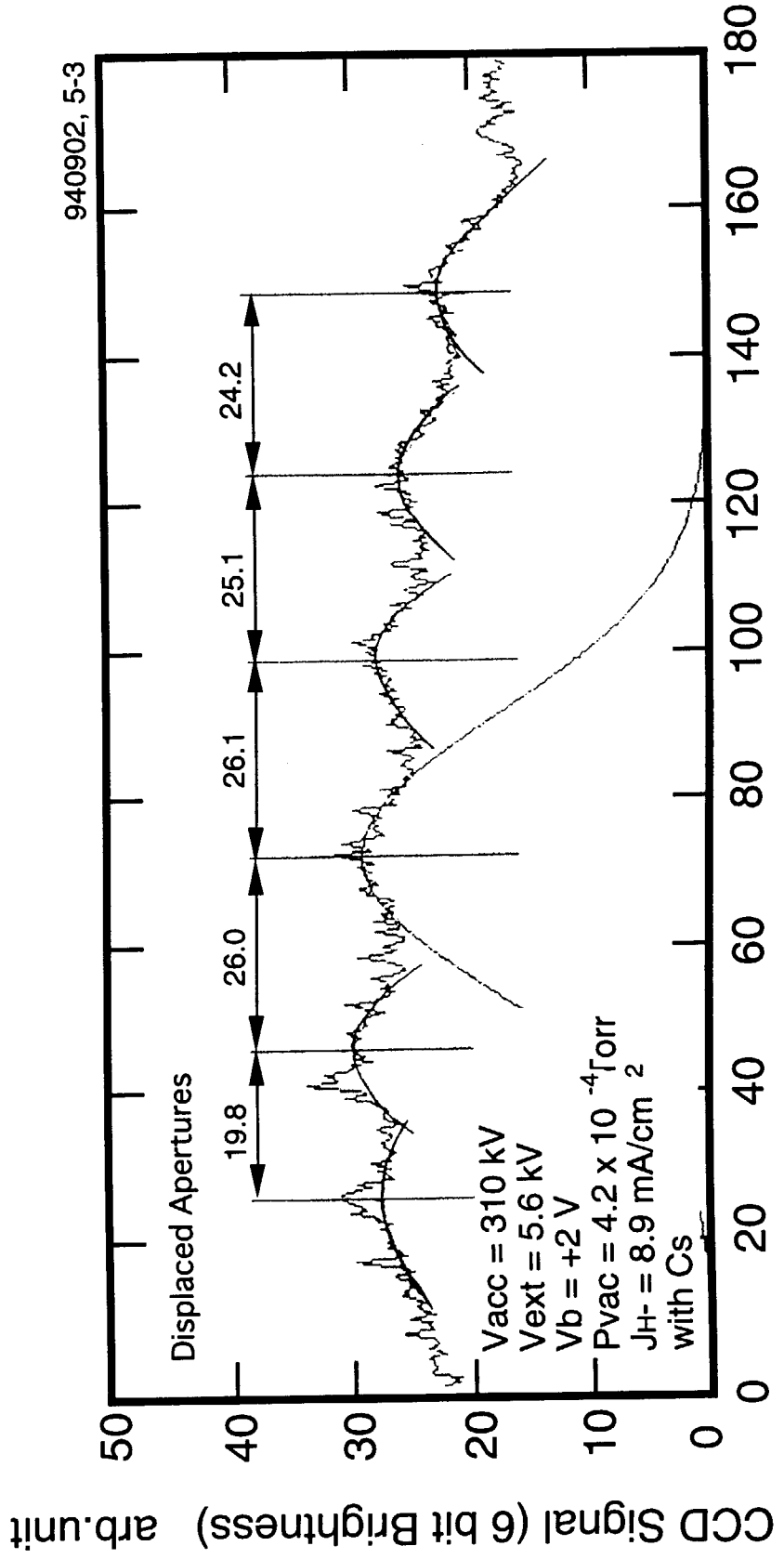

Fig. 7. A profile of the beamlets produced from a line of displaced apertures.

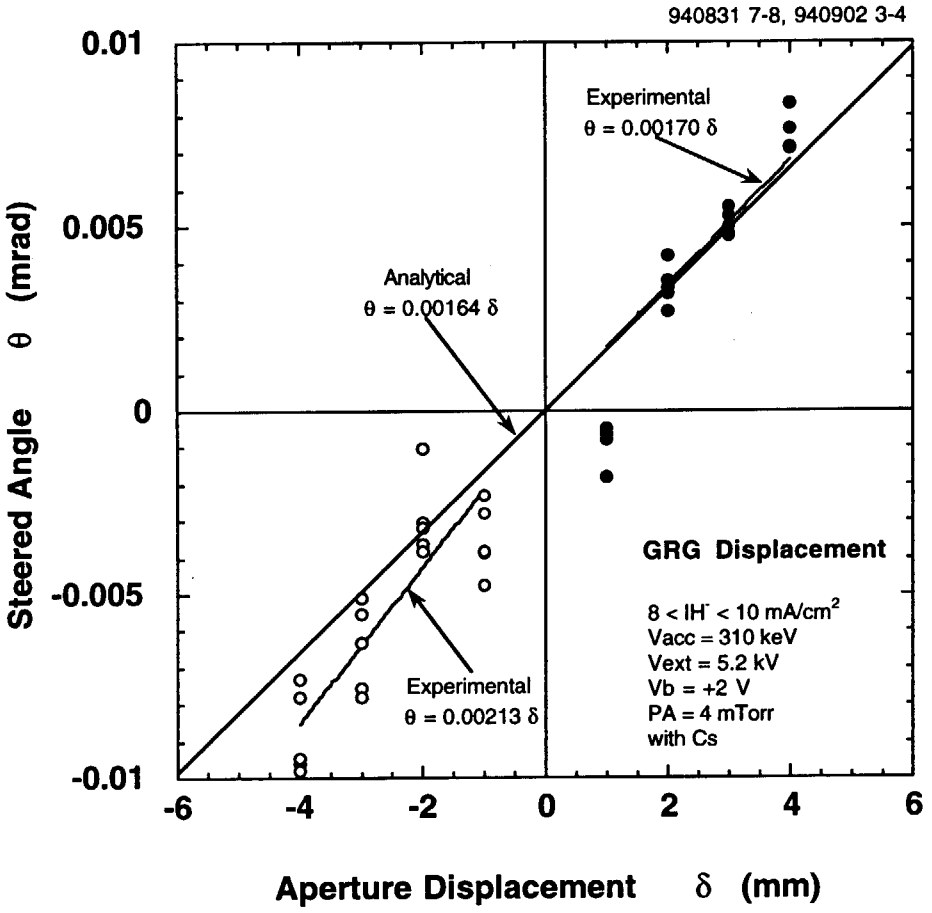

Fig. 8. The steering angle obtained at a beam energy of 310 keV as a function of the aperture displacement. An analytical result obtained with the thin lens theory is also drawn in the figure.

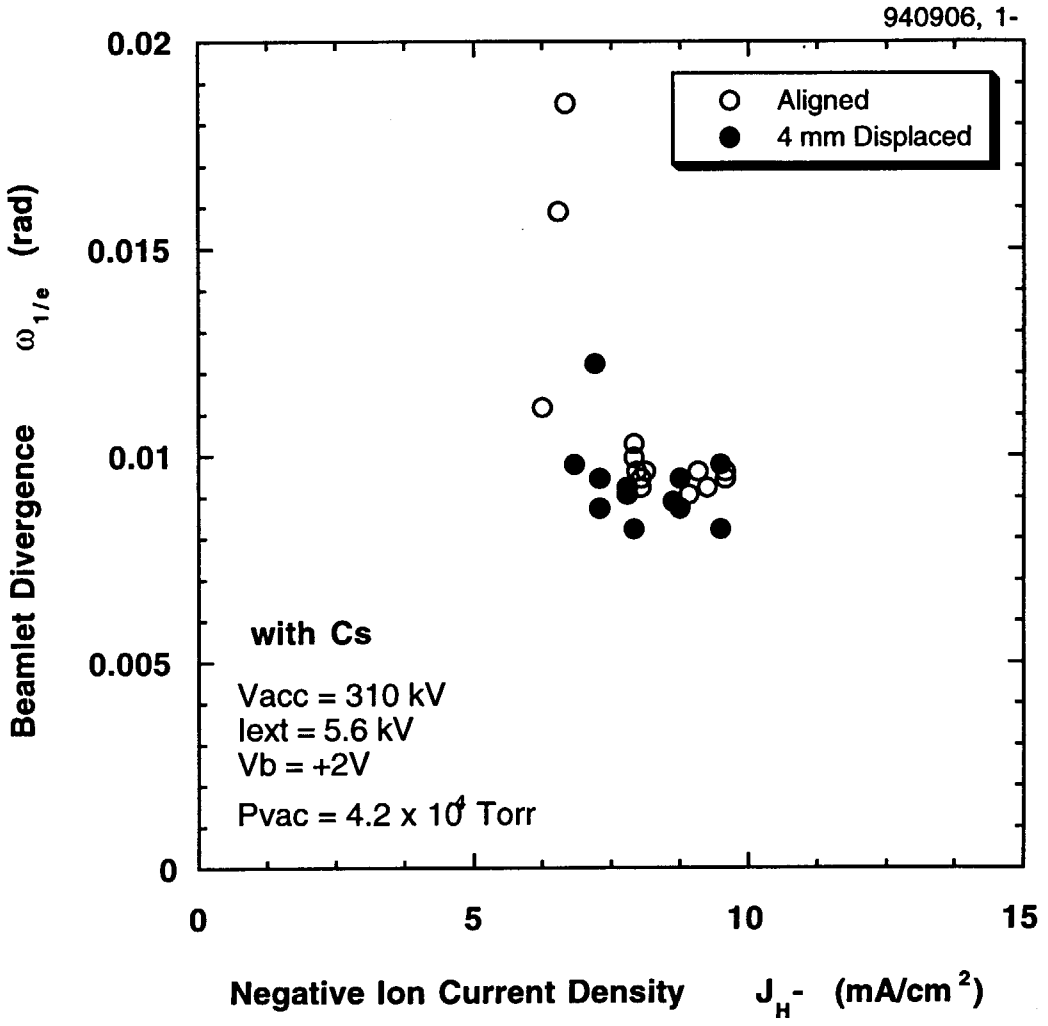

Fig. 9. The beamlet divergence obtained from aligned and displaced (δ = 4 mm) in GRG as functions of negative ion current.

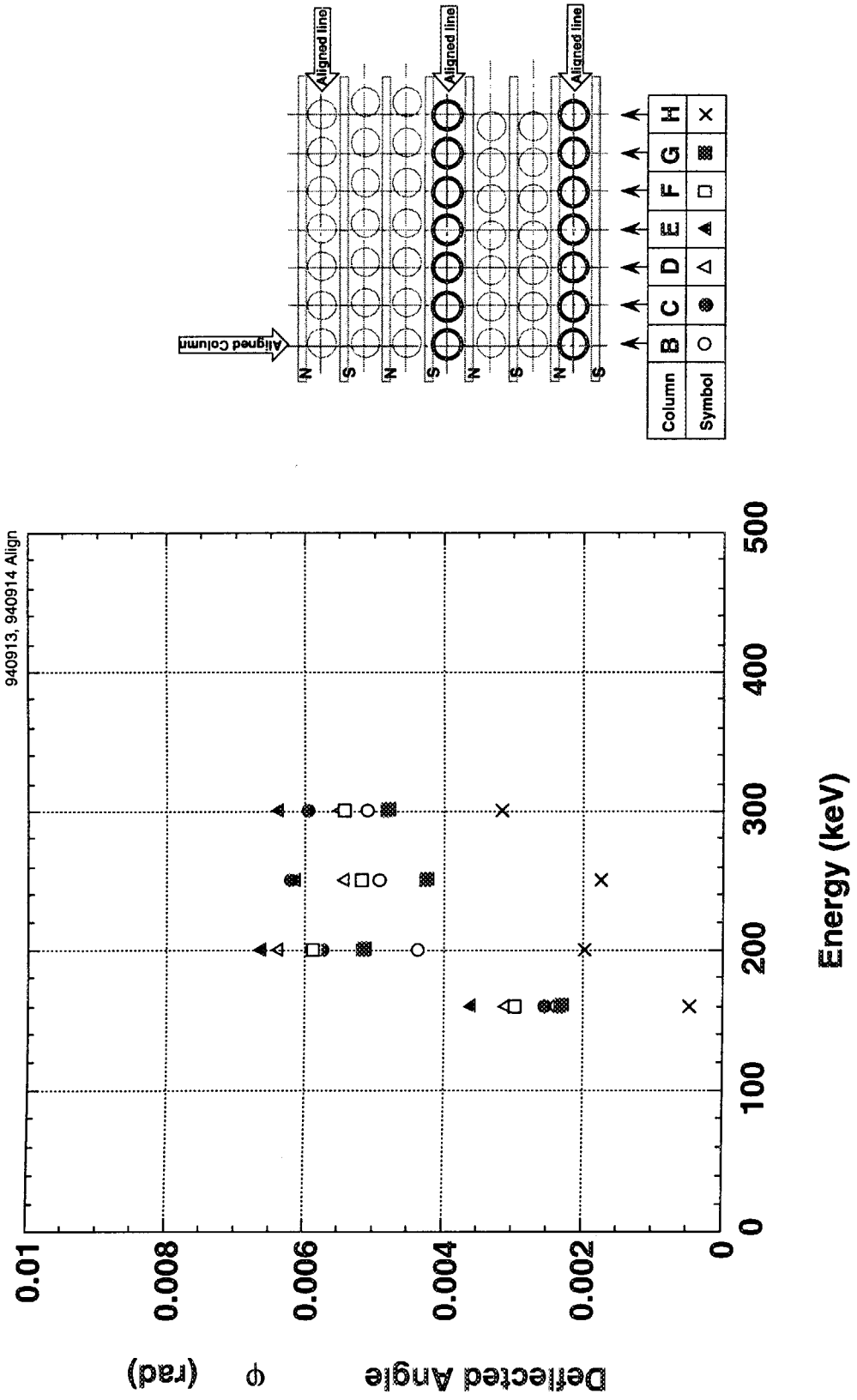

Fig. 10. The deflection angle measured at various beam energies. The symbols denote the columns of the aperture, where the beams were produced, in the grid aperture arrangement.

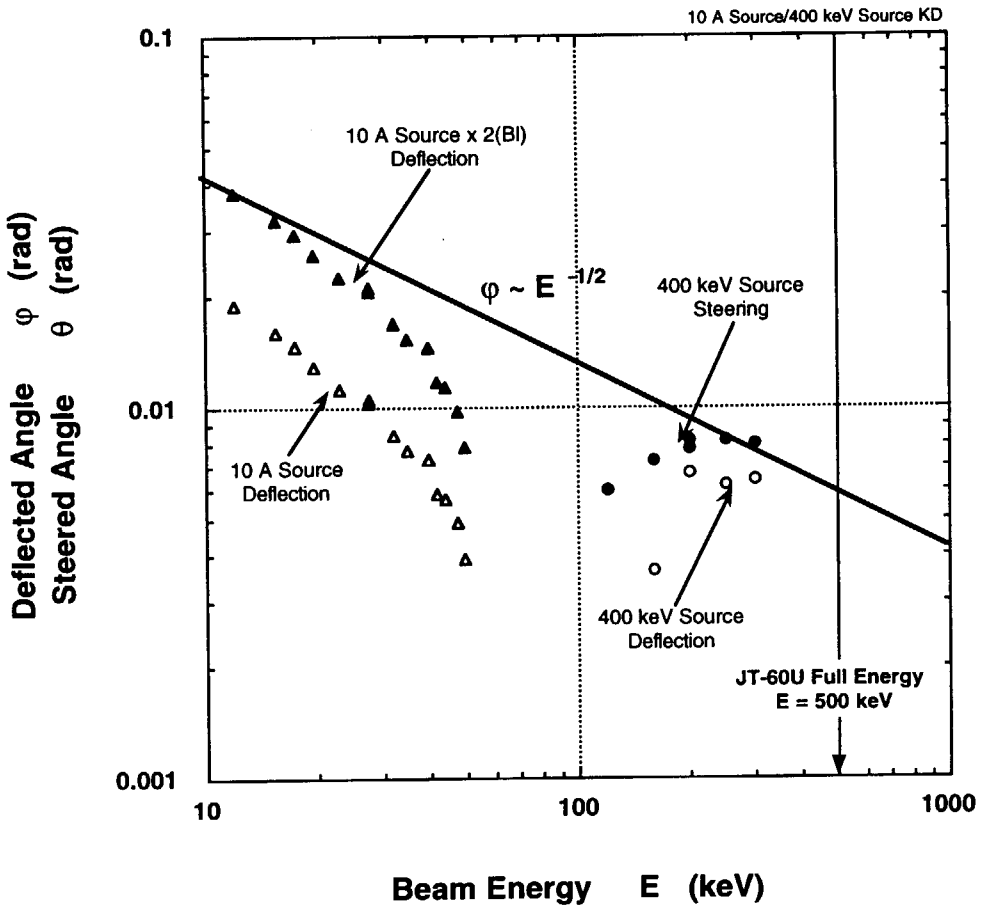

Fig. 11. The log plot of Fig. 10. The data points obtained in column E is shown in open circle.

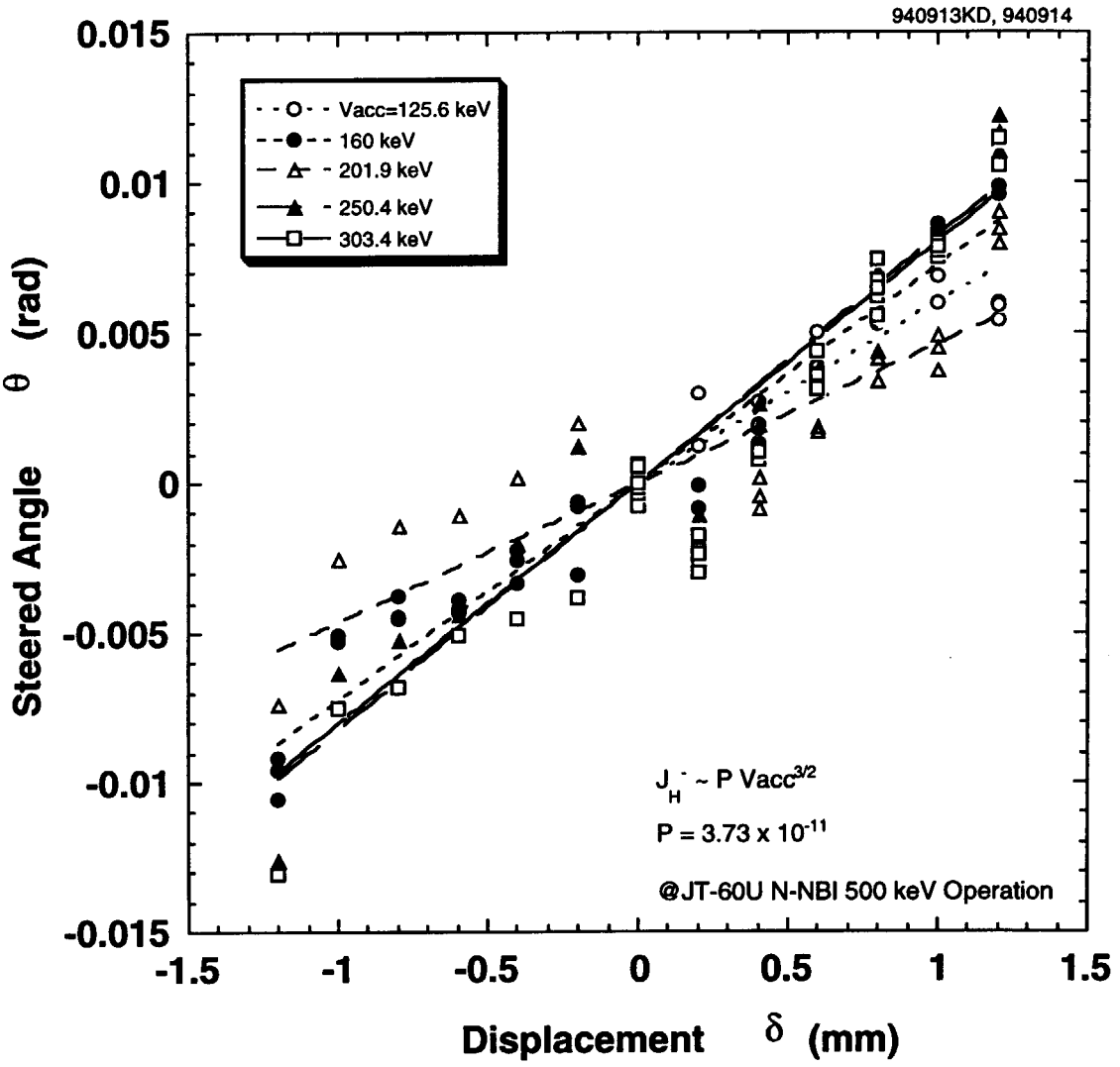

Fig. 12. The steering angle is shown in Fig. 12 as a function of the displacement for various beam energy.

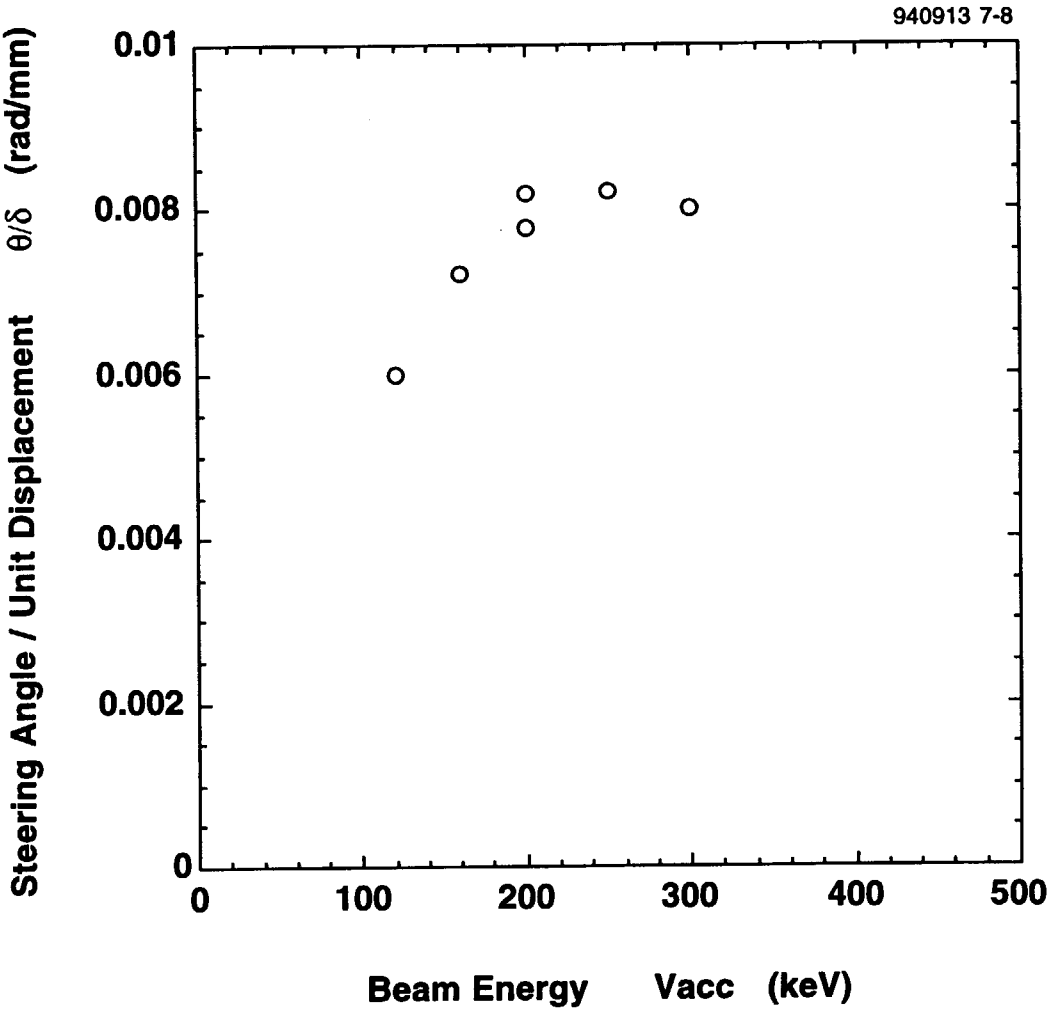

Fig. 13. The steering angle by ESG displacement for unit displacement obtained from slopes of the fitting line in Fig. 12.

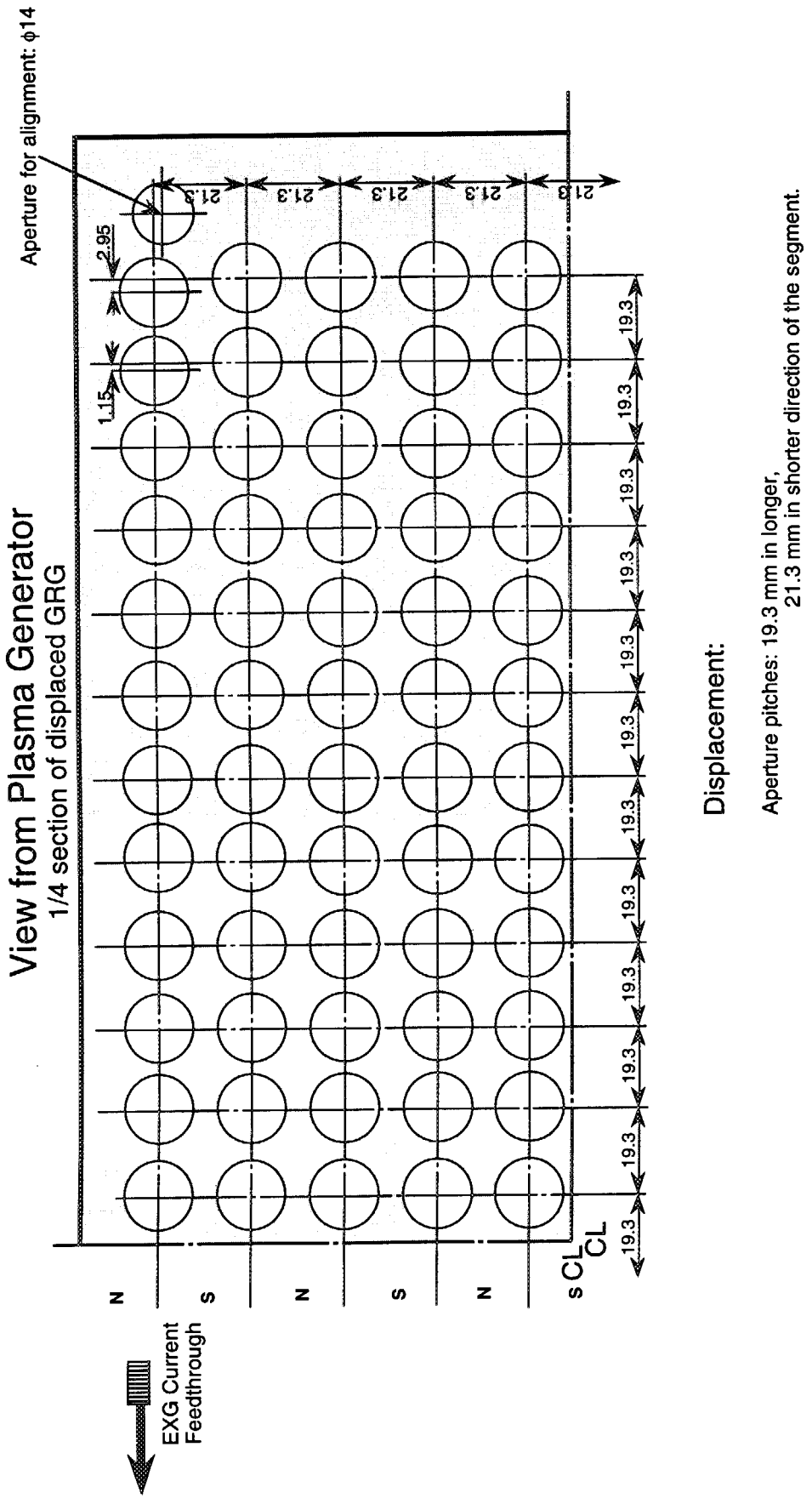

Fig. 14. The aperture arrangement of GRG in a segment designed for JT-60U source.

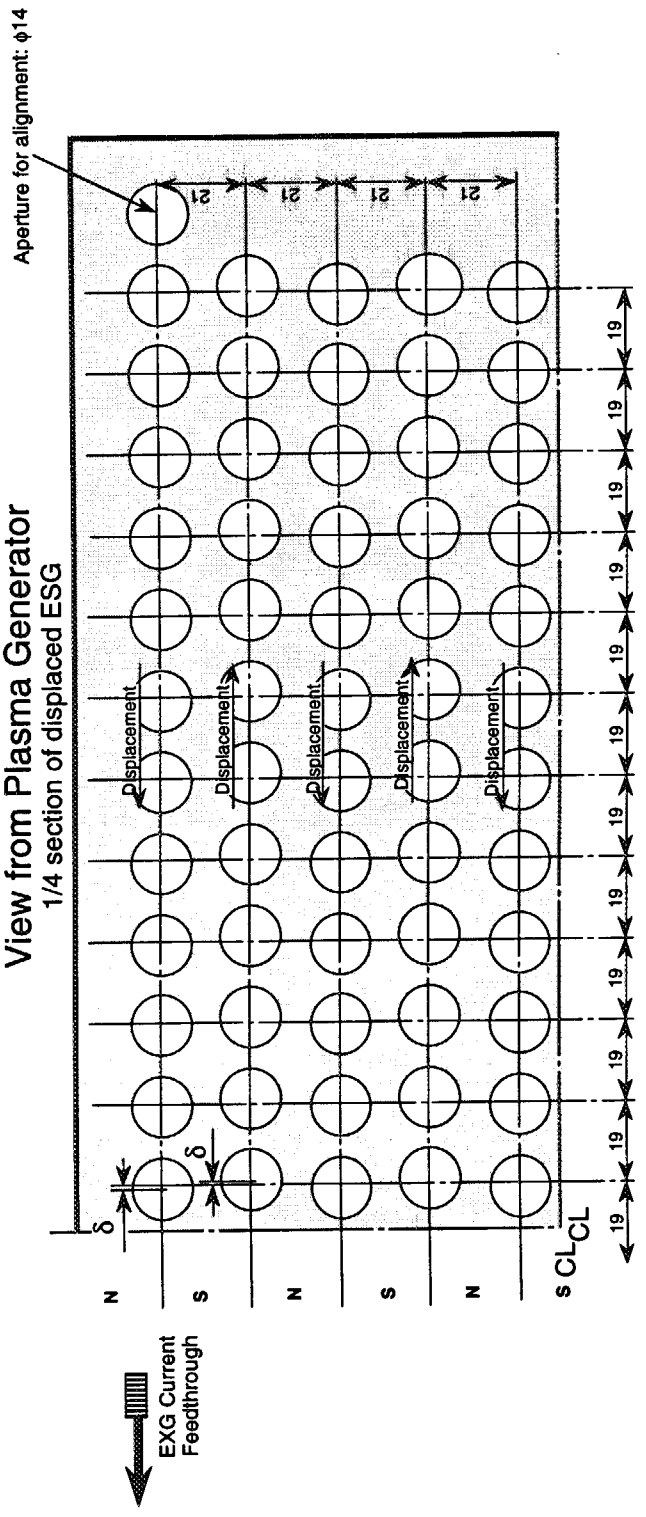

Fig. 15. The aperture arrangement of ESG in a segment designed for JT-60U source.

This is a blank page.

国際単位系 (SI) と換算表

表 1　SI 基本単位および補助単位

量	名称	記号
長さ	メートル	m
質量	キログラム	kg
時間	秒	s
電流	アンペア	A
熱力学温度	ケルビン	K
物質量	モル	mol
光度	カンデラ	cd
平面角	ラジアン	rad
立体角	ステラジアン	sr

表 2　SI と併用される単位

名称	記号
分，時，日	min，h，d
度，分，秒	°，′，″
リットル	l，L
トン	t
電子ボルト	eV
原子質量単位	u

$1\ \mathrm{eV} = 1.60218 \times 10^{-19}\ \mathrm{J}$

$1\ \mathrm{u} = 1.66054 \times 10^{-27}\ \mathrm{kg}$

表 5　SI 接頭語

倍数	接頭語	記号
10^{18}	エクサ	E
10^{15}	ペタ	P
10^{12}	テラ	T
10^{9}	ギガ	G
10^{6}	メガ	M
10^{3}	キロ	k
10^{2}	ヘクト	h
10^{1}	デカ	da
10^{-1}	デシ	d
10^{-2}	センチ	c
10^{-3}	ミリ	m
10^{-6}	マイクロ	μ
10^{-9}	ナノ	n
10^{-12}	ピコ	p
10^{-15}	フェムト	f
10^{-18}	アト	a

表 3　固有の名称をもつ SI 組立単位

量	名称	記号	他の SI 単位による表現
周波数	ヘルツ	Hz	s^{-1}
力	ニュートン	N	$m \cdot kg/s^2$
圧力，応力	パスカル	Pa	N/m^2
エネルギー，仕事，熱量	ジュール	J	N·m
工率，放射束	ワット	W	J/s
電気量，電荷	クーロン	C	A·s
電位，電圧，起電力	ボルト	V	W/A
静電容量	ファラド	F	C/V
電気抵抗	オーム	Ω	V/A
コンダクタンス	ジーメンス	S	A/V
磁束	ウェーバ	Wb	V·s
磁束密度	テスラ	T	Wb/m^2
インダクタンス	ヘンリー	H	Wb/A
セルシウス温度	セルシウス度	℃	
光束	ルーメン	lm	cd·sr
照度	ルクス	lx	lm/m^2
放射能	ベクレル	Bq	s^{-1}
吸収線量	グレイ	Gy	J/kg
線量当量	シーベルト	Sv	J/kg

表 4　SI と共に暫定的に維持される単位

名称	記号
オングストローム	Å
バーン	b
バール	bar
ガル	Gal
キュリー	Ci
レントゲン	R
ラド	rad
レム	rem

$1\ \text{Å} = 0.1\ \mathrm{nm} = 10^{-10}\ \mathrm{m}$

$1\ \mathrm{b} = 100\ \mathrm{fm}^2 = 10^{-28}\ \mathrm{m}^2$

$1\ \mathrm{bar} = 0.1\ \mathrm{MPa} = 10^5\ \mathrm{Pa}$

$1\ \mathrm{Gal} = 1\ \mathrm{cm/s}^2 = 10^{-2}\ \mathrm{m/s}^2$

$1\ \mathrm{Ci} = 3.7 \times 10^{10}\ \mathrm{Bq}$

$1\ \mathrm{R} = 2.58 \times 10^{-4}\ \mathrm{C/kg}$

$1\ \mathrm{rad} = 1\ \mathrm{cGy} = 10^{-2}\ \mathrm{Gy}$

$1\ \mathrm{rem} = 1\ \mathrm{cSv} = 10^{-2}\ \mathrm{Sv}$

（注）

1. 表 1－5 は「国際単位系」第 5 版，国際度量衡局 1985 年刊行による。ただし，1 eV および 1 u の値は CODATA の 1986 年推奨値によった。
2. 表 4 には海里，ノット，アール，ヘクタールも含まれているが日常の単位なのでここでは省略した。
3. bar は，JIS では流体の圧力を表わす場合に限り表 2 のカテゴリーに分類されている。
4. EC 閣僚理事会指令では bar，barn および「血圧の単位」mmHg を表 2 のカテゴリーに入れている。

換　算　表

力	N(=10^5dyn)	kgf	lbf
	1	0.101972	0.224809
	9.80665	1	2.20462
	4.44822	0.453592	1

粘度　$1\ \mathrm{Pa \cdot s} (\mathrm{N \cdot s/m^2}) = 10\ \mathrm{P}$（ポアズ）$(\mathrm{g/(cm \cdot s)})$

動粘度　$1\ \mathrm{m^2/s} = 10^4\ \mathrm{St}$（ストークス）$(\mathrm{cm^2/s})$

圧力	MPa(=10 bar)	kgf/cm²	atm	mmHg(Torr)	lbf/in²(psi)
	1	10.1972	9.86923	7.50062×10^3	145.038
	0.0980665	1	0.967841	735.559	14.2233
	0.101325	1.03323	1	760	14.6959
	1.33322×10^{-4}	1.35951×10^{-3}	1.31579×10^{-3}	1	1.93368×10^{-2}
	6.89476×10^{-3}	7.03070×10^{-2}	6.80460×10^{-2}	51.7149	1

エネルギー・仕事・熱量	J(=10^7erg)	kgf·m	kW·h	cal(計量法)	Btu	ft·lbf	eV
	1	0.101972	2.77778×10^{-7}	0.238889	9.47813×10^{-4}	0.737562	6.24150×10^{18}
	9.80665	1	2.72407×10^{-6}	2.34270	9.29487×10^{-3}	7.23301	6.12082×10^{19}
	3.6×10^6	3.67098×10^5	1	8.59999×10^5	3412.13	2.65522×10^6	2.24694×10^{25}
	4.18605	0.426858	1.16279×10^{-6}	1	3.96759×10^{-3}	3.08747	2.61272×10^{19}
	1055.06	107.586	2.93072×10^{-4}	252.042	1	778.172	6.58515×10^{21}
	1.35582	0.138255	3.76616×10^{-7}	0.323890	1.28506×10^{-3}	1	8.46233×10^{18}
	1.60218×10^{-19}	1.63377×10^{-20}	4.45050×10^{-26}	3.82743×10^{-20}	1.51857×10^{-22}	1.18171×10^{-19}	1

1 cal = 4.18605 J（計量法）
= 4.184 J　（熱化学）
= 4.1855 J（15 °C）
= 4.1868 J（国際蒸気表）

仕事率　1 PS（仏馬力）
= 75 kgf·m/s
= 735.499 W

放射能	Bq	Ci
	1	2.70270×10^{-11}
	3.7×10^{10}	1

吸収線量	Gy	rad
	1	100
	0.01	1

照射線量	C/kg	R
	1	3876
	2.58×10^{-4}	1

線量当量	Sv	rem
	1	100
	0.01	1

（86 年 12 月 26 日現在）

STEERING OF HIGH ENERGY NEGATIVE ION BEAM AND DESIGN OF BEAM FOCUSING/DEFLECTION COMPENSATION FOR JT-60U LARGE NEGATIVE ION SOURCE